Model for the Welding of Axial Magnetic Field Vacuum Interrupter Contacts

Erik D. Taylor, Andreas Lawall, Paul G. Slade*
Siemens AG, Rohrdamm 88, Berlin, 13629 Germany
* Consultant, Ithaca, NY 14850 U.S.A.

***Abstract*- Vacuum interrupters are required to perform a wide variety of roles within vacuum circuit breakers. One duty is to pass short-circuit currents with the vacuum interrupters' contacts closed for a period of time (1 to 4 seconds), after which the circuit breaker's mechanism must be able to open the contacts, Thus the possibility of contact welding must be minimized. The flow of current through practical contacts generates a repulsive blow-off force, which has to be balanced by a closing force from the circuit breaker mechanism plus the force from atmospheric pressure acting on the vacuum interrupter's bellows. The magnitude of the applied closing force is an important parameter in a vacuum circuit breaker's design. Axial magnetic field (AMF) vacuum interrupters have an additional attractive force because of the parallel currents flowing in the two AMF coils. This force is calculated using three-dimensional finite element analysis (FEA) for practical AMF designs using contact diameters ranging from $62 - 100\ mm$. These results are then compared to two dimensional FEA models and analytic formulas, including the effect of the current frequency on the results (DC vs. $50\ Hz$). These attractive forces can then be combined with the other forces acting on the closed vacuum interrupter contacts to calculate the threshold welding current: the current above which the contacts will form a weld. Calculations of the total closing force compare the difference in the threshold welding current between AMF and other VI contact designs.**

I. INTRODUCTION

Vacuum interrupters (VI's) must perform a wide variety of roles for the successful operation of a vacuum circuit breaker or vacuum contactor. Although high-current interruption and dielectric behavior garner most of the research focus, other duties including passing short-circuit and load currents without contact welding, the switching of capacitive and inductive loads, and the thermal behavior under normal current levels are all also critical [1]. Circuit breakers and reclosers are coordinated to allow the breaker closest to the fault to switch off during a failure event, thereby isolating the damaged section of the network while also minimizing the amount of the network without electrical power. This coordination requires that upstream circuit breakers be able to allow the short-circuit current to flow through the closed VI contacts for a period of up to a few seconds, without the contacts welding or otherwise being damaged.

When electrical contacts are closed, the current flows between the contacts through a limited set of small diameter regions where the two contacts actually touch. The transition from the current flow in the broad area contacts to the small, often millimeter diameter, region connecting the two contacts generates a blow-off between the contacts that pushes the contacts apart. The blow-off force F_B with one region of contact is given by [2]

$$F_B = \frac{\mu_0\, i^2}{4\,\pi} log_e\left(\frac{R}{a}\right) \tag{1}$$

where i is the peak current, R is the radius of the bulk contact, a is the Holm radius which is the average radius around the individual contact spots, and $\mu_0 = 4\pi \times 10^{-7}\ N/A^2$. This repulsive force can be substantial during short-circuit currents. F_B can reduce the net force applied to the contacts, thereby increasing the contact resistance and leading to contact welding when the contacts locally melt. If F_B larger than the applied force, the contacts can separate and produce an arc. This arc can locally melt the contacts, producing a weld when the contacts come back together.

II. THEORY OF THRESHOLD CURRENT FOR WELDING

The application of Eq. (1) is often limited due to a lack of detailed knowledge about the size, number and distribution of contact regions. The possibility of more than one contact region is well established; arc visualization experiments with vacuum interrupters have observed up to seven parallel arcs during contact opening [3], for example. The collection of experimental data for the repulsion or blow-off force on closed contacts produced an empirical relationship for this force [4]

$$F_B = \beta \cdot i^2 \tag{2}$$

where $\beta = 4.8 \times 10^{-7}\ N/A^2$. The data used to derive this empirical formula covers a period of 65 years, and includes data from contacts in both air and in vacuum with currents ranging from $1 - 200\ kA\ peak$.

The threshold current i_W where welding begins to occur is [5]

$$i_W = \frac{2\,U_m\,\sqrt{n}\,\sqrt{F}}{\{\rho^2 \cdot \pi\, 0.1\,H_0 + 4\,U_m^2\,(\beta - k\,n)\}^{1/2}} \qquad (3)$$

where

$$\rho = \rho_0 \left(1 + \frac{2}{3}\,\alpha\,(T_1 - T_0)\right) \qquad (4)$$

and where U_m is the melting voltage, n is the number of contact regions, F is the externally applied force, H_0 is the contact material hardness at room temperature, k is a term quantifying the attractive force between AMF coils, ρ_0 is the contact material resistivity at temperature T_0, $\alpha = 3.5 \times 10^{-3}\ 1/°K$ is the temperature coefficient of resistivity, and T_1 is the temperature at the contact spot. This model is further discussed and developed in [6, 7, 8].

Equation 3 is based on calculating the current where the melting voltage U_m is reached. At this point, the local contact area melts and welding begins. The factors in Eq. (3) affect the resistance in the contact point; a higher resistance requires a lower current to reach U_m. The various terms in Eq. (3) represent the balance of different effects on the resistance of the contact spot including the base resistivity of contact material, along with the effects of heating from the high current flow on increasing the resistivity. The material hardness is also influenced by the heating of the contact spot by the current. As the temperature increases, the hardness will correspondingly decrease, thereby reducing the resistance. The force externally applied to the contacts F reduces the resistance. The term β determines how much the blow-off reduces the net force. The one remaining piece of the puzzle is the attractive force between AMF coils, represented by the factor k in Eq. (3). This force acts against the blow-off force, and reduces the additional force required to prevent welding. This is discussed in the next section.

III. Modeling of Attractive Force in AMF

The axial magnetic field (AMF) coils used for arc control in VI's are fundamentally two loops of current, with the current flowing in the same direction, as shown in Fig. 1. This configuration produces an attractive force F_A between the coils. The simplest formula uses the attractive force per length between two infinite wires, multiplied by the circumference of the coils

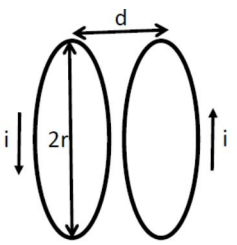

Fig. 1: two coils with an attractive force due to the parallel current flow in each loop.

$$F_A = \frac{\mu_0\,r\,i^2}{d} \qquad (5)$$

where r is the radius of the coils, and d is the distance between the two coils.

An improved analytic model solves for the attractive force of two current carrying rings. The attractive force is [9]

$$F_A = \frac{\mu_0\,i^2\,\kappa\,d}{4\,r} \cdot \left[\frac{2-\kappa^2}{1-\kappa^2} \cdot E(\kappa) - 2\,K(\kappa)\right] \qquad (6)$$

where

$$\kappa = \sqrt{\frac{4\,r^2}{4\,r^2 + d^2}} \qquad (7)$$

$K(\kappa)$ and $E(\kappa)$ are elliptical integrals of the 1st and 2nd kind

$$K(\kappa) = \int_0^{\pi/2} \frac{d\alpha}{\sqrt{1 - \kappa^2 \cdot sin^2(\alpha)}} \qquad (8)$$

$$E(\kappa) = \int_0^{\pi/2} \sqrt{1 - \kappa^2 \cdot sin^2(\alpha)}\,d\alpha \qquad (9)$$

Although Eqs. (6) through (9) appear complicated, it is straightforward to program these equations into any of a variety of symbolic calculation programs to determine F_A using Eq. (6).

Both Eqs. (5) and (6) have the same general form of

$$F_A = k \cdot i^2 \qquad (10)$$

where k depends only on the geometry of the particular coil arrangement. Equation (10) also generally applies to two and three dimensional modeling of the attractive force, where the force scales as the square of the peak current, and the proportionality constant is a function of the geometry. This modeling includes some aspects of the physical size of an actual AMF coil, as well as the effects of eddy currents in the contacts between the two coils, as in Fig. 2. For initial comparison to the analytic formula Eq. (6), the two dimensional modeling is first performed with a constant current (0 Hz). This model shows the effects of the physical dimensions of the coils and their positions.

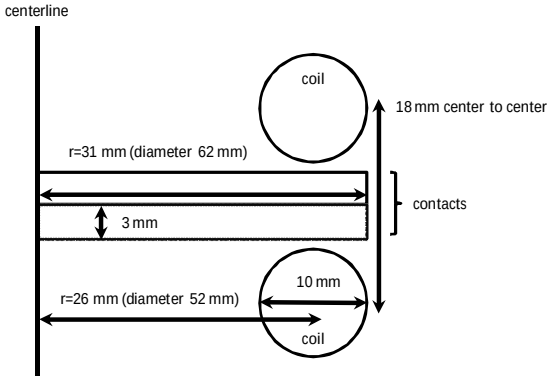

Fig. 2: structure used for two-dimensional axi-symmetric modeling; the 62mm diameter case is shown.

Fig. 3: coil structure used for three-dimensional model. Current path indicated by arrows. 62 mm diameter case shown.

The main effect is a reduction of the attractive force. Once a value of k is found using Eq. (5), Eq. (6), or FEA modeling, this value can be inserted into Eq. (3) to calculate the threshold welding current.

The 3-D FEA model includes the actual structure of the AMF coils, the contacts, support post behind the contacts and the portion of the terminals near to the coils. The AMF coils have the cup coil arrangement with six arms, as described in [10] and shown in Fig. 3. The force in the axial direction on the coil, support post and terminal on one side is calculated to determine the attractive force. The net force on all parts is also calculated to be zero, thereby helping to verify the model setup. The attractive force is modeled for three contact diameters, 62, 90 and 100 mm. A peak current of $56.6\,kA$ ($40\,kA\,rms$) is used for each model. In order to compare 3-D model with the two dimensional model, the peak current is divided by the number of arms of the actual AMF contact structure (i.e. 6) for the two dimensional model: the current flowing in the 2-D ring is $\sqrt{2}\cdot 40\,kA/6 = 9.4\,kA$.

The results of the analytic formulas and the two dimensional modeling are shown in Fig. 4, which plots the attractive forces as a function of the external diameter of the AMF. Since Eqs. (5) and (6) treat the AMF coils as if they were a thin wire, the radius and coil spacing should at the center of the current distribution in the coil. For example, the coil structure

Table I: The attractive force F_A based on the three-dimensional modeling in Fig. 4, and the constant k from Eq. 10 based on these calculations.

$d\ [mm]$	$F_A\ [N]$	$k\ [N/A^2]$
62	253	7.9×10^{-8}
90	268	8.4×10^{-8}
100	285	8.9×10^{-8}

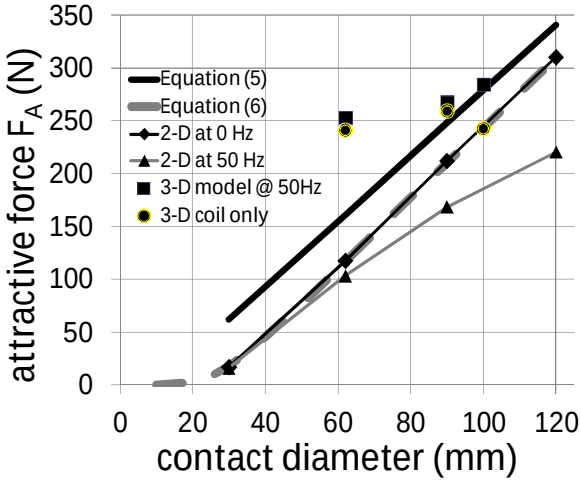

Fig. 4: Comparison of the analytic Eqs (5) and (6) with two-dimensional modeling using the general structure shown in Fig. 2 at 0 and 50 Hz, and three-dimensional modeling of the general structure in Fig. 3 at 50 Hz.

in Fig. 4, the external coil radius r is 31 mm ($diameter = 62\,mm$), and the diameter used to calculate the radius is reduced by $10\,mm$ with $r = (diameter - 10\,mm)/2$. With this correction to r, the analytic model in Eq. (6) of current rings agrees very well with the two dimensional modeling at 0 Hz.

The results of the three dimensional modeling at 50 Hz for the 62, 90, and 100 mm AMF coils are also plotted in Fig. 4. The plot includes both the total axial force on the contact, coil structure, and the terminal on one side, and the force contribution from the AMF coil alone. The total attractive forces for the 3-D AMF model are higher than the values from either the analytic formulas or the two dimensional modeling. These calculated values are summarized in Table I.

IV. DISCUSSION

The attractive force in the axial direction comes from the azimuthal current density j_θ and the radial magnetic field B_r integrated over the coil

$$F_A = \int j_\theta \cdot B_r \, dV \qquad (11)$$

Looking at a single coil in open space, the magnetic pinch force acts on the coil. This generates a force that attempts to compress the coil towards the center of the current path. Although the magnitude of the force can be significant near the surface the coil (where B_r is largest), the net force on the coil averages to zero, giving no overall axial motion for the coil. The addition of a second coil gives an additional B_r component in the first coil, thereby leading to the attractive force from Eqs. (5) and (6) and the two-dimensional modeling. However, the distance between the coils d reduces the magnitude of the resulting attractive force.

In realistic AMF coils, features like the overlapping coil arms in cup-shaped AMF coils can create an additional B_r term, which then modifies the attractive force. Other contact structures that could modify the attractive force include portions of the current path where the current flow area expands or contracts. This is seen in the difference between the total force and force on the AMF coils alone.

The attractive force can provide a non-trivial increase in the threshold welding current for a given design contact force. Non-AMF arrangements would generally have $k = 0$. Using Eq. (3) for Cu-Cr contacts with 3 regions of contact, a diameter of 62 mm and $\rho = 33\,\mu\Omega \cdot mm$, $\alpha = 3.5 \times 10^{-3}$, $n = 3$, $U_m = 0.43\,V$ and $H_0 = 700\ N/mm^2$. The design force is $4020\,N$ and the added force from atmospheric pressure on the vacuum interrupter's bellows is $230\,N$ giving $F = 4250\,N$ for a fault current of $40\,kA\,rms$. For example: For the TMF contact $i_W = 56.7\,kA$, but for the AMF contact $i_W = 59.5\,kA$, an increase of $1.8\,kA$.

The threshold welding current given in Eq. (3) refers to the point where contact welding begins to occur. Unfortunately it is not always feasible to apply enough force to completely eliminate contact welding. Most circuit breakers use a hammer force on contact opening that is sufficient to break a certain level of contact welding. In addition, certain contact materials such as Ag-WC and Cu-W are specifically designed to resist the formation of welds and/or readily fracture when a hammer force is applied to welded contacts [11], allowing them to open. Future work can focus on performing this analysis using the actual peak current values that are interrupted with a given contact diameter. Future work could also focus on characterizing the strength of welds that do occur as a function of the current above i_W, and connect this to either a static force required to break weld and/or the dynamic hammer force to break the weld.

V. Conclusions

The force applied to vacuum interrupter contacts by the circuit breaker serves to reduce the resistance at the contact points, and hence serves to increase the threshold welding current i_W. Two factors can change the net force applied to the contacts: the blow-off force from the current constriction at the surface, and the attractive force between the axial magnetic field (AMF) coils. This attractive force can be estimated using analytical equations and two-dimensional FEA modeling. These estimates were compared to the calculations from three-dimensional models of the system. The comparison shows that although the analytical and two-dimensional models are useful as a guide, the determination of the constant k requires a three-dimensional simulation of the actual geometry.

References

[1] P. G. Slade, *The Vacuum Interrupter: Theory, Design, and Application*, New York: CRC Press, 2008.

[2] R. Holm, *Electric Contacts: Theory and Application*, New York:Springer-Verlag, 1967.

[3] T. Lamara, D. Gentsch, "Theoretical and experimental investigation of new innovative TMF-AMF contacts for high current vacuum arc interruption," *IEEE Trans. Plasma Sci*., vol. 41, no. 8, pg. 2043, Aug. 2013.

[4] E. D. Taylor, P. G. Slade, "The Repulsion or Blow-Off Force Between Closed Contacts Carrying Current," *Proc. 62nd Holm Conf. Electrical Contacts*, 2016.

[5] P. G. Slade, E. D. Taylor, A. Lawall, "The Threshold Welding Current for Closed Vacuum Interrupter Contacts with 'n' Regions of Contact for Short Duration, High Fault Currents," *Proc. 28th ICEC Int. Conf. Electrical Contacts*, 2016.

[6] P. G. Slade, "The current level to weld closed contacts," *Proc. 59th Holm Conf. Electrical Contacts*, 2013, pg. 123.

[7] P. G. Slade, "The Threshold Welding Current for Large Area Closed Contacts with Two or Three points of Contact," *Proc. 27th ICEC Int. Conf. Electrical Contacts*, 2014, pg. 17.

[8] P. G. Slade, "The Contact Force to Prevent Large Area, Closed, Vacuum Interrupter Contacts from Welding when Passing High Fault Currents of up to 4 Seconds," *Proc. 61st Holm Conf. Electrical Contacts*, 2015, pg. 95.

[9] S. I. Babic, C. Akyel, "Magnetic force calculation between thin coaxial circular coils in air," *IEEE Trans. Magn*., vol. 44, no. 4, pg. 445, April 2008

[10] B. J. Paul, R. Renz, "Contact arrangement for vacuum switches," U. S. Patent 4,620,074, 28 Oct. 1986.

[11] P. G. Slade, "Advances in Material Development for High Power, Vacuum Interrupter Contacts," *IEEE Trans. Comp., Packag., Manufact. Technol. A*, vol. 17, pp. 96, March 1994.